SAE TECHNICAL PAPER SERIES

2008-36-0059

E

DOI: 10.4271/2008-36-0059

Reliable TDC position determination: a comparison of different thermodynamic methods through experimental data and simulations

Emiliano Pipitone
Department of Mechanics, University of Palermo, Italy

Alberto Beccari
Department of Mechanics, University of Palermo, Italy

Stefano Beccari
Department of Mechanics, University of Palermo, Italy

SAE BRASIL
Sociedade de Engenheiros da Mobilidade

FILIADA À
SAE International

Congresso 2008
SAE BRASIL

XVII Congresso e Exposição Internacionais da Tecnologia da Mobilidade
São Paulo, Brasil
07 a 09 de outubro de 2008

2008-36-0059

Reliable TDC position determination: a comparison of different thermodynamic methods through experimental data and simulations

Emiliano Pipitone
Alberto Beccari
Stefano Beccari
Department of Mechanics, University of Palermo, Italy

ABSTRACT

It is known to internal combustion researcher that the correct determination of the crank position when the piston is at Top Dead Centre (TDC) is very important, since an error of 1 crank angle degree (CAD) can cause up to a 10% evaluation error on indicated mean effective pressure (IMEP) and a 25% error on the heat released by the combustion: the TDC position should be then known within a precision of 0.1 CAD. This task can be accomplished by means of a dedicated capacitive sensor, which allows a measurement within the required 0.1 degrees precision. Such a sensor has a substantial cost and its use is not really fast; a different approach can be followed using a thermodynamic method, whose input is the pressure curve sampled during the compression and expansion strokes of a "motored" (i.e. without combustion) cylinder.

In this work the authors compare an original thermodynamic method with other ones available in literature, by means of both experimental and simulated pressure curves. A zero dimensional thermodynamic model was employed to obtain an extensive collection of numeric pressure curves by changing engine geometry (e.g. compression ratios from 10 to 20 were adopted), operative conditions and wall heat transfer laws. The in-cylinder mass leakage has been taken into account in the model.

Moreover, in order to assess the reliability and robustness of each method, the typical measurement errors and disturbances related to indicating analysis have been taken into account. The capability of the investigated methods to provide the correct TDC position in presence of the above mentioned errors has been evaluated.

INTRODUCTION

In-cylinder pressure analysis is of great importance in R&D of internal combustion engines, since it allows the evaluation of many important parameters, such as IMEP, mean friction pressure, indicated fuel consumption, heat release rate or mass fraction burned. It is also known that the exact determination of the crank position when the piston is at TDC is of vital importance, since an error of 1 CAD can cause up to a 10% evaluation error on IMEP and a 25% error on the heat released by the combustion: the TDC position should be then known within the precision of 0.1 CAD. This task can be accomplished by means of a dedicated capacitive sensor, which allows a dynamic measurement (i.e. while the cylinder is motored) within the required 0.1 degrees precision. Such a sensor has a substantial cost and its use is not really fast, since it must be fitted in the spark plug or injector hole of the motored cylinder. A different approach can be followed using a thermodynamic method, whose input is the pressure curve sampled during the compression and expansion strokes of a "motored" (i.e. without combustion) cylinder. Different thermodynamic methods for the evaluation of the TDC position can be found in literature. Some of them only require, as input, the measure of the in-cylinder pressure curve during the compression and expansion strokes in a motored cylinder, giving as output the TDC location. Others are instead characterized by a more complex and time consuming implementation, since the calibration of an engine model through some constants or coefficients (e.g. the heat exchange coefficient) is mandatory for every single engine studied. The four thermodynamic methods here considered for the comparison all belong

to the first category and are here listed together with their authors:

Method n. 1: Beccari, Pipitone [1];
Method n. 2: Tazerout, Le Corre, Rousseau [2];
Method n. 3: Stas [3];
Method n. 4: Nilsson, Eriksson [4].

In the following section a brief description is given for each of the methods considered.

MAIN SECTION

The first of the methods considered is an original procedure proposed by the authors of the present paper and relies on the study of the so called "*loss function*"(*F*), i.e. a function expressly defined which takes into account the effect, on the in-cylinder pressure change, of the heat transfer and the mass leakage: both of them are in fact responsible for the so called "*loss angle*" (ϑ_{loss}), which is the angular phase lag between the location of peak pressure (LPP) and the TDC location (LTDC) and is caused both by heat transfer and mass leakage. The method can be applied through the following steps [1]:

1. The phase of the pressure cycle is adjusted by setting the LPP at zero CAD : in this way the position error is exactly equal to the unknown loss angle

2. Evaluation of the angular position ϑ_1 and ϑ_2 of the minimum and maximum relative volume change $\delta V/V$, for example using the following equation [1]

$$\vartheta_{1,2} = \mp 76.307 \cdot \mu^{0.123} \cdot \rho^{-0.466}$$

where ρ is the engine compression ratio while μ is the rod to crank ratio, V is the cylinder volume and δV the volume change due to a crank rotation $\delta\vartheta$ ($\vartheta=0$ corresponds to the TDC).

3. Calculus of the loss function increments δF_1 and δF_2 at the angular position ϑ_1 and ϑ_2 by means of the following equation:

$$\delta F = c_P \frac{\delta V}{V} + c_V \frac{\delta p}{p}$$

where p is the gas pressure (and hence δp represents the pressure change due to a crank rotation $\delta\vartheta$), c_p and c_v are the specific heat at constant pressure and constant volume respectively.

4. Calculus of the mean value δF_m=1/2 (δF_1+δF_2).

5. Evaluation of the loss function increment at the peak pressure position δF_{LPP} by means of the mean value δF_m through the proportionality constant E_p which can be assumed equal to 1.95 [1], hence:

$$\delta F_{LPP} = E_P \cdot \delta F_m \approx 1.95 \cdot \delta F_m$$

6. The loss angle ϑ_{loss}, and hence the TDC location, can be evaluated by means of the following equation:

$$\vartheta_{loss} = \frac{2}{\rho - 1} \cdot \frac{\mu}{\mu + 1} \cdot \left[\frac{1}{c_p} \frac{\delta F}{\delta \vartheta} \right]_{LPP}$$

Once the loss angle value is found, the LTDC can be evaluated by adding ϑ_{loss} to the LPP. This method has a general validity because it takes into account the effects of both heat exchange and mass leakage through the estimation of the loss function increment at LPP (δF_{LPP}) by means of the known functions $\delta V/V$ and $\delta p/p$. The method n. 2 is based on the analysis of the temperature-entropy (*T*-*S*) diagram of the compression and expansion strokes under the assumption of constant mass evolution (i.e. no gas leakage or blow-by). The progress of the curve in this diagram depends on the relative position between the pressure curve and the cylinder volume. The authors of the method point out that, when the pressure is correctly phased with respect to the volume, the entropy must change symmetrically with respect to the peak temperature T_{max} as in figure 1; the authors also show that, under gross TDC position errors, a loop appears in the *T*-*S* diagram (see figure 2); hence, according to them, the correct phasing between pressure and volume is reached in two steps: first, the pressure curve must be shifted until the loop disappears (figure 3) and then a further shift of -0.45 CAD should be applied to find the correct pressure curve position.

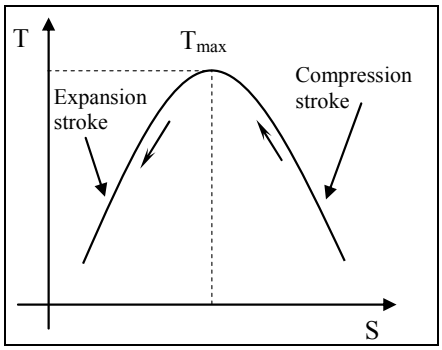

figure 1 - T-S diagram when the pressure curve is correctly phased

The method is based on some thermodynamic imprecision, since the authors, as is shown further on, implicitly affirm that the loss angle is always equal to 0.45 CAD, despite the engine geometry or the operative conditions. As is known from literature [1, 5, 6], the loss angle entity may depends on the engine characteristics and dimensions, reaching values as high as 1 CAD for large diesel engine (see figure 4). In this case this method would cause a TDC position evaluation error of 0.55 CAD, which is unacceptable.

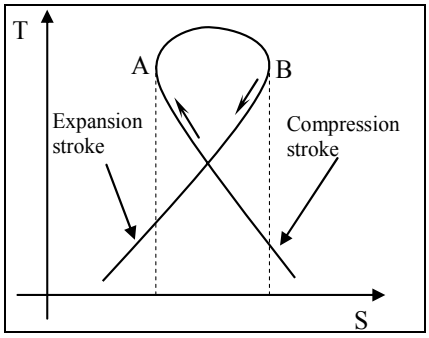

figure 2 - pressure wrongly phased so as to generate a loop in the T-S diagram

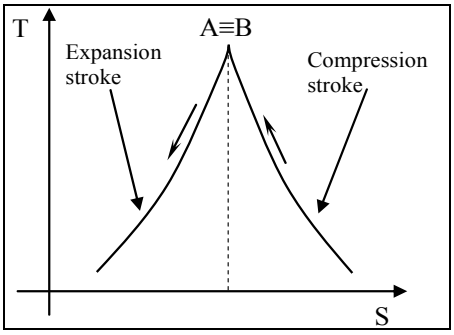

figure 3 - the loop disappears when the two points A and B coincide

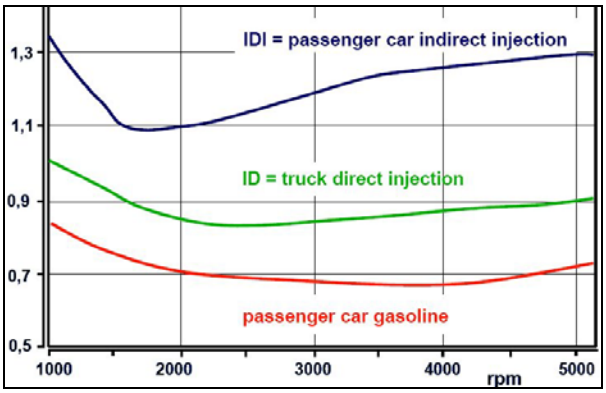

figure 4 - loss angle vs. engine speed for different engine types [5]

Here it will be shown that the loop in the *T-S* diagram disappears when the pressure cycle is phased so as to have LPP=0, i.e. when the TDC position error is equal to the whole loss angle. Taking in to account the perfect gas law for a constant mass evolution:

$$T = \frac{pV}{mR} \quad \Rightarrow \quad \frac{dT}{T} = \frac{dp}{p} + \frac{dV}{V}$$

where T, p and m, are the gas temperature, pressure and mass respectively; V and R are the cylinder volume and the gas constant. The specific entropy variation δS corresponding to a crank rotation $\delta\vartheta$, in the hypothesis of constant mass of gas in the cylinder, can be written as:

$$\delta S = \frac{\delta q}{T} = \frac{\delta u + p\delta v}{T} = \frac{\delta i - v\delta p}{T} = \\ = c_p \cdot \frac{\delta T}{T} - R\frac{\delta p}{p} = c_p \frac{\delta V}{V} + c_v \frac{\delta p}{p} \qquad (1)$$

where δq is the specific heat received by the gas during the crank rotation $\delta\vartheta$, u and i are the gas specific internal energy and enthalpy respectively. The presence of a loop in the *T-S* diagram imply the existence of two points in which δS=0 (points A and B in figure 2). The points A and B, characterised by δS=0, are also displayed in figure 5 which plots the δS function versus the crank position for different phasing errors between pressure curve and cylinder volume.

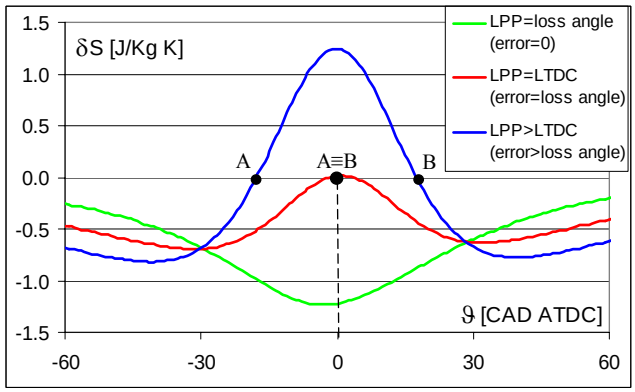

figure 5 - δS function for different phase lags between LPP and LTDC ($\delta\vartheta$=1 CAD)

When the pressure curve is back-shifted, with respect to the cylinder volume, the loop area becomes smaller, until the two points overlap (A≡B in figure 3 and figure 5) and the loop area disappears. From the analysis of the δS function (see equation (1) and figure 5) it follows that the condition A≡B is verified only when LPP≡LTDC ($\delta p/p = \delta V/V$=0) that means a pressure curve position error equal to the whole loss angle. The further shift of -0.45 CAD proposed by the authors of the method has been evaluated by means of some thermodynamic simulations, neglecting the effect of the mass leakage, which, just like the heat transfer, tends to back-shift the peak pressure location with respect to the LTDC. The error introduced by the use of this method is then the difference between the real loss angle and the fixed value 0.45 CAD. Since intrinsically incorrect and unreliable, this method has not been included in the following comparisons.

The method n. 3 is based on the analysis of the polytropic exponent values, evaluated at the pressure curve inflection points, with varying phase lag between LPP and LTDC. This method starts phasing the pressure curve so that LPP=0 CAD: then the polytropic compression and expansion coefficients, m_1 and m_2, at the pressure curve inflection points are evaluated. The inflection points fulfill the following condition:

$$\frac{\delta^2 p(\vartheta)}{\delta \vartheta^2} = 0$$

The polytropic exponents, m_1 and m_2, are evaluated by means of the following equation:

$$m_i = -\frac{\delta p_i}{\delta V_i}\frac{V_i}{p_i} \quad ; i = 1, 2 \qquad (2)$$

where p_i and V_i are the gas pressure and cylinder volume respectively, at the pressure curve inflection points, while δp_i and δV_i are the pressure and volume variations corresponding to a crank rotation $\delta\vartheta$. According to the author of the method, the pressure curve must be back-shifted with respect to the cylinder volume and the new polytropic exponents at the inflection points, m'_1 and m'_2, evaluated. The correct TDC position is found when the following equation is verified:

$$\frac{m'_2 - m'_1}{m_2 - m_1} = 2.25$$

The method n. 4 compares the compression and the expansion phases of the cylinder pressure curve focusing on two segments located between fixed crank angles (*-b, -a* and *a, b* in figure 6). The two segments are displayed in figure 6 (curves CD and EF). The authors affirm that the pressure curve is correctly phased when the segment CD, mirrored with respect to the LTDC, overlaps the segment EF. To compare the two curves a pressure offset $\Delta(\vartheta)$ must be applied to the EF segment to compensate for heat transfer occurred between angles $-a$ and a. The offset $\Delta(\vartheta)$ is:

$$\Delta(\vartheta) = \left(p(\vartheta_{TDC} - \vartheta_0) - p(\vartheta_{TDC} + \vartheta_0)\right) \cdot \left(\frac{V(\vartheta_{TDC} + \vartheta_0)}{V(\vartheta_{TDC} + \vartheta)}\right)^{\eta}$$

where p and V are the in-cylinder pressure and volume, ϑ_{TDC} is the estimated TDC location, ϑ_0 is the middle of the region [*a; b*] (see figure 6), ϑ is the generic crank angle ($a < \vartheta < b$) and η is a constant depending on the heat transfer with chamber walls [4]. The correct TDC position can be obtained minimizing the following sum of squared errors:

$$\sum_{a<\vartheta_i<b} \left\{p(\vartheta_{TDC} - \vartheta_i) - \left[p(\vartheta_{TDC} + \vartheta_i) + \Delta(\vartheta_{TDC} + \vartheta_i)\right]\right\}^2$$

As reported by the authors of the method [4], recommended values for the crank positions *a* and *b* are 30° and 115° CA respectively, while η should be set to 1.1

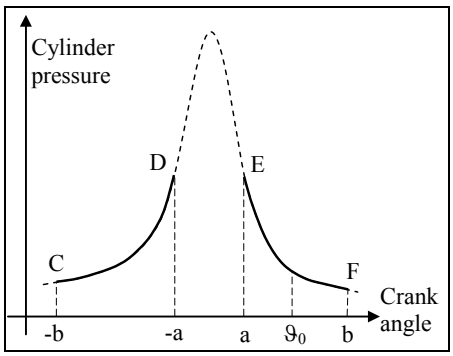

figure 6 - the two regions of the pressure curve investigated in method n. 4

EXPERIMENTAL TESTS

As a first step, the comparison between the different methods has been carried out by means of experimental data acquired on the test bed equipped with a four cylinder spark ignition engine, whose characteristics are resumed in Table 1, connected to an eddy current dynamometer. The pressure cycle of a motored cylinder has been sampled by means of an AVL GU13X pressure transducer, fitted on its spark plug adaptor AVL ZC32, under different operative conditions of engine speed (from 1500 to 3000 rpm with increments of 500 rpm) and Manifold Absolute Pressure (MAP, from 0.4 to 0.6 bar with increments of 0.1 bar). In order to overcome the cycle-by-cycle variations, which may affects indicating analysis even under motored conditions, 100 consecutive pressure curves have been acquired for each operative condition, each curve corresponding to an engine cycle (720 CAD); the three selected thermodynamic methods have been applied to each curve and the mean result evaluated together with the scattering.

Table 1 - Engine geometry

Displacement [litre]	1.242
Bore [mm]	70.80
Stroke [mm]	78.86
Compression ratio ρ	9.8
Rod to crank ratio μ	3.27

The engine TDC location has been measured, in the same operative conditions, by means of a Kistler 2629B capacitive sensor, whose accuracy is 0.1 CAD. Both in-cylinder pressure and TDC sensor output were sampled, with 1 CAD sampling rate, using a 360 ppr

encoder to trigger and clock the acquisition performed using a National Instrument PCI-6133 DAQ board.

The 1 CAD sampling rate could appear inadequate to obtain the required 0.1 CAD accuracy for the TDC position determination; hence, in order to verify the reliability of acquisition performed, the TDC sensor signal has been acquired using an Agilent 100MHz oscilloscope with the resolution of 0.045° crank rotation. The same signal has been down-sampled with 1 CAD resolution and interpolated, in a range of 7 CAD around the maximum, by means of a 4th order polynomial, which was then used to compute the location of the maximum, obtaining the same TDC location of the original curve sampled at 0.045° resolution (a tolerance of 0.01 CAD was reached). The same procedure was followed at different engine speed, obtaining always a quite good matching of the TDC positions. This demonstrates, in the authors' opinion, that a 1 CAD sampling rate allows the estimation of the TDC position with the required accuracy of 0.1 degrees. The same procedure was applied to in-cylinder pressure curves using a 3rd order fitting polynomial, confirming the capability to locate the peak pressure with the same accuracy of 0.1 degrees.

In method n. 1, a 3rd degree polynomial was also used to fit the $\delta p/p$ values in a range of ±20 CAD around the two locations corresponding to the minimum and maximum $\delta V/V$: this procedure corresponds to a low-pass filtering that eliminates the high frequency noise, allowing a reliable evaluation of the loss function increment (δF).

In method n. 3 the pressure curve inflection point positions are calculated by means of the second derivative evaluation that is strongly influenced by the presence of high frequency noise, for this reason a polynomial fit has been employed to filter the pressure values near the inflection point locations.

The experimental pressure curves have been analyzed by means of methods n. 1, 3 and 4 and the results, in terms of TDC position error with respect to the measured value, are reported in Table 2, together with the measured loss angles. As shown, the best LTDC prediction is obtained by means of method n.1 with a mean error, over the different operative conditions, of -0.15 CAD. A slightly worse result is obtained by the use of both methods n. 3 and n. 4 with a mean error of -0.21 and 0.19 CAD respectively. As already pointed out, method n.2 would give the worst result with a mean error of 0.35 CAD (=0.80-0.45). As concern the scattering, the worst result is shown by the method n.3 with a value of ±0.32 CAD while the other two methods show a scattering of about ±0.1 CAD. It's worth mentioning that both methods n.1 and 3 show a better LTDC prediction at lower engine speed (see figure 7), since they predict decreasing loss angles with increasing engine speed, while the experimental data, reported in Table 2, show an almost constant loss angle for different operative conditions: this is effectively predicted by the method n. 4 which shows the nearly constant error of 0.2 CAD. Hence methods n.1 and 3 give the best result at engine speed not higher than 2000 rpm. In conclusion, the three compared methods show an acceptable LTDC prediction (with mean errors in the range of ±0.2 CAD).

Table 2 - TDC position errors evaluated by means of the three thermodynamic methods

			LTDC evaluation errors [CAD ATDC]		
Engine speed [rpm]	**MAP [bar]**	**actual loss angle**	**method n. 1**	**method n. 3**	**method n. 4**
1500	0.4	-0.82	-0.06	0.09	0.18
1500	0.5	-0.79	-0.01	0.10	0.24
1500	0.6	-0.79	-0.06	0.06	0.17
2000	0.4	-0.81	-0.14	-0.16	0.13
2000	0.5	-0.72	-0.07	-0.11	0.18
2000	0.6	-0.7	-0.06	-0.06	0.15
2500	0.4	-0.9	-0.26	-0.55	0.26
2500	0.5	-0.85	-0.19	-0.39	0.18
2500	0.6	-0.79	-0.21	-0.35	0.19
3000	0.4	-0.8	-0.23	-0.32	0.09
3000	0.5	-0.79	-0.23	-0.42	0.29
3000	0.6	-0.79	-0.31	-0.41	0.18
mean		**-0.80**	**-0.15**	**-0.21**	**0.19**
scattering		**±0.10**	**±0.15**	**±0.32**	**±0.10**

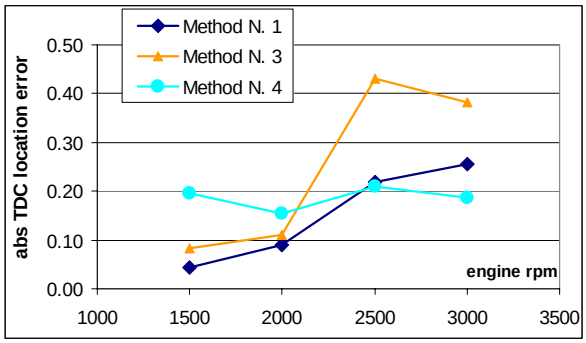

figure 7 - mean TDC location error as function of engine speed

ROBUSTNESS TESTS

In the second part of the work, the authors aimed to test the robustness of the three thermodynamic methods to the most frequent pressure measurement

errors and disturbances, by the use of numeric pressure curves.

In order to obtain the pressure curves corresponding to the compression and expansion strokes, some thermodynamic simulations have been performed by means of a zero dimensional thermodynamic model realized on a spreadsheet with a resolution of 1 crank angle degree. The model was based on the first law of thermodynamics, which allows calculating the pressure variation of the gas (air) due to in-cylinder volume changes during both the compression and expansion strokes:

$$\delta q - p\delta v = \delta u \qquad (3)$$

where δq represents the specific heat received by the gas from the cylinder walls during the crank rotation $\delta\vartheta$, p and v represent the gas pressure and specific volume, and δu the specific internal energy variation. The gas involved in the process can be assumed to be a perfect gas, thus the following equations are also valid:

$$\left.\begin{array}{c} pv = R'T \Rightarrow \dfrac{dp}{p} + \dfrac{dv}{v} = \dfrac{dT}{T} \\ \delta u = c_v \delta T \end{array}\right\} \qquad (4)$$

being T the gas temperature and R' the gas constant. Due to the mass leakage through the piston rings and the valve seats, the available volume V for the in-cylinder gas increases, hence the specific volume changes:

$$V = v \cdot m \quad \Rightarrow \quad \frac{dv}{v} = \frac{dV}{V} - \frac{dm}{m} \qquad (5)$$

where m represents the in-cylinder mass. From equations (3), (4) and (5) the in cylinder pressure variation δp due to a crank rotation $\delta\vartheta$ is:

$$\delta p = \frac{1}{V}\left[\delta Q(k-1) - kp\delta V\right] + kp\frac{\delta m}{m} \qquad (6)$$

where k is the isentropic coefficient $=c_P/c_V$, and δm represents the mass entering the cylinder during the crank rotation $\delta\vartheta$ (hence the mass leakage is characterized by $\delta m<0$). In the thermodynamic model both c_P and c_V where considered function of the gas temperature by means of the equation valid for air:

$$c_p = 1403.06 - 360.72\cdot\left(\frac{1000}{T}\right) + 108.24\cdot\left(\frac{1000}{T}\right)^2 - 10.79\cdot\left(\frac{1000}{T}\right)^3$$

$$c_v = c_p - R' \qquad R' = 287.1 \qquad k = \frac{c_p}{c_v}$$

Two different heat transfer models have been considered, in order to test the methods robustness:

a) the Woschni model [7, 8]

$h=3.26\cdot d^{-0.2}(2.28\,u_m)^{0.8}T^{-0.53}p^{0.8}$ [W/m^{2}K]

d = cylinder bore [m]
T = gas temperature [K]
p = gas pressure [kPa]
u_m = mean piston speed [m/s]

b) the Eichelberg model [7, 9]

$h=2.43u_m^{0.33}(pT)^{0.5}$ [W/m^{2}K]

T = gas temperature [K]
p = gas pressure [bar]
u_m = mean piston speed [m/s]

It's worth to mention that in the listed heat transfer models, any term related to the combustion pressure has been omitted, since the task is to simulate the pressure changes in a motored engine. Once fixed the model, the heat received by the gas during the time interval δt (i.e. in the rotation arc $\delta\vartheta$) can be evaluated as:

$$\delta Q = h\cdot\Delta T\cdot A\cdot\delta t = h\cdot\Delta T\cdot A\cdot\frac{\delta\vartheta}{\omega}$$

being ω the engine speed [rad/sec], $\Delta T=T_{wall}-T$ the temperature difference between the cylinder walls and the gas, A the instantaneous in-cylinder wall surface.

Gas leakage has been modeled as the mass flowing through an equivalent convergent nozzle; hence in the time interval δt the mass δm can be evaluated as:

$$\delta m = -G_{nozzle}\cdot\delta t = -G_{nozzle}\cdot\frac{\delta\vartheta}{\omega} \qquad (7)$$

where the mass flow G_{nozzle} depends on the in-cylinder pressure p and on the outer pressure p_{out}:

$$G_{nozzle} = \begin{cases} A_N\sqrt{\dfrac{2k}{k-1}m\dfrac{p}{V}\left[\left(\dfrac{p_{out}}{p}\right)^{\frac{2}{k}} - \left(\dfrac{p_{out}}{p}\right)^{\frac{k+1}{k}}\right]} & if\left(\dfrac{p_{out}}{p}\right) > \left[\dfrac{p_{out}}{p}\right]_{CR} \\ A_N\sqrt{km\dfrac{p}{V}\left(\dfrac{2}{k+1}\right)^{\frac{k+1}{k-1}}} & if\left(\dfrac{p_{out}}{p}\right) \le \left[\dfrac{p_{out}}{p}\right]_{CR} \end{cases}$$

being $\left[\dfrac{p_{out}}{p}\right]_{CR} \approx 0.53$

Here A_N represents the equivalent flow area, which has been estimated by-means of the results exposed in [10] keeping a constant proportionality with the piston surface area. The crank rotation taken into consideration in the simulation ranges from -180 to +180 CAD ATDC, with neither inlet valve lag angle nor advanced opening of exhaust valve. The simulations were carried out, as resumed in Table 3, taking into consideration the dimensions of a commercial available automotive engine, three compression ratios (10, 16 and 20), different conditions of MAP and speed and employing the two heat transfer models above mentioned.

Table 3 - Engine geometry and simulation parameters

Manifold absolute pressure	0.4 to 1.0 bar (steps of 0.1)
Engine speed	1000 to 3000 rpm (steps of 500)
Compression ratio (ρ)	10, 16 and 20
Rod to crank ratio (μ)	3.27
Bore	70.80 mm
Stroke	78.86 mm
Air temperature at IVC	35° C
Walls temperature	70° C
Heat transfer model	Woschni (ρ = 10, 16, 20) Eichelberg (ρ = 16, 20)

As already mentioned, one of the purposes of the present papers is to asses the robustness of the methods toward the most common in-cylinder pressure measurement errors or disturbances, which are:

1. Pressure bias error: this kind of error is present when a dynamic or an un-cooled piezoelectric sensor is used. If the pressure curve is compensated by means of one of the most known methods [11, 12], the pressure evaluation uncertainties may be as high as ±10 kPa.
2. Engine compression ratio: this parameter is normally known with some approximation, typically ±3%. Such uncertainty may introduce an estimation error on the evaluation of in-cylinder volume, which in turn may affect the reliability of the tested methods.
3. Gas temperature: during the compression-expansion process it can be evaluated by means of the perfect gas law, once known the gas temperature at inlet valve closure T_{IVC}, which is usually determined on the base of the manifold gas temperature with an error as high as ±30°C.
4. Pressure measurement noise: a noise component is always present in the pressure signal measured. It may origin from the mechanical vibrations perceived by the transducer or from electromagnetic interferences. Analyzing some experimental pressure cycles sampled on a spark ignition engine, it was found that the intensity of such a noise typically reaches a 600 Pascal standard deviation. Depending on its origin, the noise may be amplified together with the pressure signal, so its amplitude may change with the pressure range, which is obviously related to the compression ratio ρ. For this reason, in the simulations performed, the noise amplitude has been assumed to be 600 Pa when ρ is equal to 10 (S.I. engine), 1200 Pa for ρ = 16 (S.I. CNG engine or C.I. engine) and 1800 Pa for ρ = 20 (C.I. engine).

The pressure curves obtained by the simulations, for each of the operative conditions resumed in Table 3, were modified introducing the above mentioned measurement errors as described in the following equations:

$$p' = p + p_{bias} + p_{noise}$$
$$T'_{IVC} = T_{IVC} + error_T$$
$$\rho' = \rho \cdot \left(1 + error_\rho\right)$$

On a first step the measurement errors were introduced one at a time, then the resulting pressure, volume and temperature data were employed to compute the loss angle by means of the thermodynamic methods. Table 4 and Table 5 report the LTDC evaluation error for each of the disturbances introduced. The tables contain the maximum error resulting from the analysis of the 35 pressure curves obtained by the thermodynamic simulation in the operative conditions of Table 3.

As scan be seen, method n. 1 seems to give the best results in all the investigated conditions, allowing to evaluate the TDC position with a maximum error of 0.11 CAD. Methods n. 3 and 4 give worse results since the maximum TDC estimation error is 0.20 and 0.39 CAD respectively. In particular the method n. 4 returns unacceptable errors for compression ratio equal to 10 and Woschni model.

In a real experimental test, however, the above mentioned disturbances may occur all simultaneously. Hence, in order to assess the robustness of the methods under the worst possible condition, the pressure cycles simulated in the 35 operative conditions of Table 3 (this time only the Woschni model and two compression ratios were considered) were modified using the combination of disturbances resumed in Table **6**, Table 7 and Table 8 and then employed to determine the loss angle by means of the three methods. Obviously the uncertainty on the in-cylinder gas temperature has not been considered for the methods n.3 and 4, since it has no effect in the LTDC evaluation.

Table 4 - Maximum LTDC evaluation error of each method (Woschni heat transfer model)

	Max. LTDC error [CAD ATDC]			
ρ = 10	Disturbance entity	**Method n. 1**	**Method n. 3**	**Method n. 4**
No disturbance		0.030	0.164	0.330
T_{IVC}	+30°C	0.029	0.164	0.330
T_{IVC}	−30°C	0.031	0.164	0.330
Compression ratio	+5%	-0.044	0.201	0.390
Compression ratio	−5%	0.085	0.133	0.270
Pressure bias error	+10 kPa	0.023	0.161	0.330
Pressure bias error	−10 kPa	0.058	0.167	0.330
Pressure signal noise	st. dev. 600 Pa	0.041	-0.175	0.387
ρ = 16				
No disturbance		-0.040	0.112	0.094
T_{IVC}	+30°C	-0.042	0.112	0.094
T_{IVC}	−30°C	-0.036	0.112	0.094
Compression ratio	+5%	-0.077	0.135	0.117
Compression ratio	−5%	0.060	0.090	-0.082
Pressure bias error	+10 kPa	-0.045	0.111	0.094
Pressure bias error	−10 kPa	-0.035	0.113	0.094
Pressure signal noise	st. dev. 1200 Pa	-0.064	0.093	0.102
ρ = 20				
No disturbance		-0.042	0.090	-0.142
T_{IVC}	+30°C	-0.042	0.090	-0.142
T_{IVC}	−30°C	-0.043	0.090	-0.142
Compression ratio	+5%	-0.082	0.115	-0.110
Compression ratio	−5%	0.027	-0.106	-0.176
Pressure bias error	+10 kPa	-0.056	0.089	-0.142
Pressure bias error	−10 kPa	-0.033	0.090	-0.142
Pressure signal noise	st. dev. 1800 Pa	-0.114	-0.090	-0.083

The maximum TDC position errors, obtained for each disturbances combination, are presented in Table 6, Table 7 and Table 8 both for low and high compression ratio. As shown the method n. 1 provides, once more, a reliable TDC prediction even in presence of all the disturbances; the worst result corresponds to an evaluation error 0.146 CAD obtained for ρ =10. Considering that the above disturbance values are overestimated with respect to the real ones, the method shows a good robustness to measurement errors.

Table 5 - Maximum LTDC evaluation error of each method (Eichelberg heat transfer model)

	Max LTDC error [CAD ATDC]			
ρ= 16	Disturbance entity	**Method n. 1**	**Method n. 3**	**Method n. 4**
No disturbance		0.018	0.144	0.127
T_{IVC}	+30°C	0.023	0.144	0.127
T_{IVC}	−30°C	0.021	0.144	0.127
Compression ratio	+5%	-0.067	0.186	0.144
Compression ratio	−5%	0.075	0.104	0.108
Pressure bias error	+10 kPa	-0.022	0.142	0.127
Pressure bias error	−10 kPa	0.033	0.145	0.127
Pressure signal noise	st. dev. 1200 Pa	-0.090	-0.094	0.169
ρ= 20				
No disturbance		-0.038	0.099	-0.146
T_{IVC}	+30°C	-0.037	0.099	-0.146
T_{IVC}	−30°C	-0.033	0.099	-0.146
Compression ratio	+5%	-0.088	0.136	-0.105
Compression ratio	−5%	0.048	-0.087	-0.191
Pressure bias error	+10 kPa	-0.048	0.098	-0.146
Pressure bias error	−10 kPa	0.023	0.100	-0.146
Pressure signal noise	st. dev. 1800 Pa	-0.106	-0.087	-0.113

Table 6 - Disturbances combination and maximum LTDC evaluation errors for method n. 1

Pressure signal noise	st. dev. 600 Pa (ρ=10) or 1800 Pa (ρ=20)			
T_{IVC} error	−30°C			
Compression ratio error	−5%		+5%	
Pressure bias error [kPa]	−10	+10	−10	+10
max LTDC error (compression ratio = 10)	0.130	0.081	-0.107	-0.128
max LTDC error (compression ratio = 20)	-0.059	-0.072	-0.119	-0.133

T_{IVC} error	+30°C			
Compression ratio error	−5%		+5%	
Pressure bias error [kPa]	−10	+10	−10	+10
max LTDC error (compression ratio = 10)	0.146	0.080	-0.107	-0.146
max LTDC error (compression ratio = 20)	-0.043	-0.085	-0.109	-0.140

Table 7 - Disturbances combination and LTDC evaluation errors for method n. 3

Pressure signal noise	st. dev. 600 Pa (ρ=10) or 1800 Pa (ρ=20)			
Compression ratio error	−5%		+5%	
Pressure bias error [kPa]	−10	+10	−10	+10
max LTDC error (compression ratio = 10)	-0.196	-0.206	-0.144	-0.154
max LTDC error (compression ratio = 20)	-0.113	-0.113	0.100	0.099

Table 8 - Disturbances combination and LTDC evaluation errors (method n. 4)

Pressure signal noise	st. dev. 600 Pa (ρ=10) or 1800 Pa (ρ=20)			
Compression ratio error	−5%		+5%	
Pressure bias error [kPa]	−10	+10	−10	+10
max LTDC error (compression ratio = 10)	0.328	0.328	0.445	0.445
max LTDC error (compression ratio = 20)	-0.117	-0.117	0.090	0.090

Method n. 3 shows a slightly worse TDC prediction, with errors up to 0.206 CAD, while method n. 4 gives unacceptable errors (as high as 0.445 CAD) for low compression ratio simulations.

CONCLUSIONS

In this paper four thermodynamic methods for the determination of the TDC position have been taken into consideration in order to make a comparison on the base of both experimental tests and simulations. One of the method (the n. 2), as a result of some imprecision in its base theory, revealed to be incorrect and unreliable and therefore has been excluded by the comparison. The first part of the comparison was carried out through the use of experimental pressure cycles acquired on the engine test bed and showed that the three remaining methods effectively determine the TDC position with acceptable approximation, i.e. with error lower than 0.2 CAD. The second part of the comparison aimed to test the robustness of the methods trough the use of pressure curve obtained by means of thermodynamic simulations of the in-cylinder compression-expansion process for different operative condition of manifold pressure and engine speed. The methods robustness has been put to the test by the implementation, in the numeric pressure curve, of the most common pressure measurement errors and disturbances. The results showed that method n. 1 provides good results also with numerical pressure curves and the TDC position evaluation error remained near the recommended value of 0.1 CAD. Method n. 3 gives also good results, even if with slightly higher errors. Method n. 4 instead, even if proved reliable with experimental data, revealed poor performances when applied to the simulated pressure curve, above all in presence of measurement errors and disturbances.

AKNOWLEDGEMENT

The authors express all their appreciation to Mr. Beniamino Drago for its invaluable technical support.

REFERENCES

1. Pipitone E., Beccari A., “Determination of TDC in internal combustion engines by a newly developed thermodynamic approach”, Appl. Therm. Eng., Vol. 30, Issues 14-15, 2010, DOI: 10.1016/ j.applthermaleng.2010.04.012.
2. Tazerout M., Le Corre O., Rousseau S., "TDC Determination in Ic Engines Based on the Thermodynamic Analysis of the Temperature-Entropy Diagram", SAE Paper 1999-01-1489.
3. Stas Marek J., "Thermodynamic Determination of TDC in Piston Combustion Engines", SAE Paper 960610.
4. Nilsson Ylva, Eriksson Lars, "Determining TDC Position Using Symmetry and Other Methods", SAE Paper 2004-01-1458.
5. www.avl.com
6. E. Pipitone, A. Beccari, S. Beccari, “The experimental validation of a new thermodynamic method for TDC determination”, SAE Technical paper 2007-24-0052, DOI: 10.4271/2007-24-0052.
7. C. A. Finol and K. Robinson, "Thermal modelling of modern engines: a review of empirical correlations to estimate the in-cylinder heat transfer coefficient", Journal of Automobile Engineering, Proc. IMechE Part D, Vol. 220, 2006
8. J.I. Ramos, “Internal combustion engine modeling”, Hemisphere Publishing Corporation, 1989
9. J.H. Horlock and D.E. Winterbone, “The Thermodynamics and gas dynamics of Internal Combustion Engines”, Volume II, Clarendon Press, Oxford 1986
10. A. Hribernik, "Statistical Determination of Correlation Between Pressure and Crankshaft Angle During Indication of Combustion Engines", SAE Paper 982541
11. Randolph Andrew L., "Methods of processing cylinder-pressure transducer signals to maximize data accuracy", SAE Paper 900170
12. Brunt Michael F. J., Pond Christopher R., "Evaluation of techniques for absolute cylinder pressure correction", SAE Paper 970036

DEFINITIONS, ACRONYMS, ABBREVIATIONS

A=instantaneous in-cylinder walls surface [m^2].
A_N = equivalent flow area [m^2].
ATDC = after TDC.
CAD = Crank Angle Degrees.
CNG = Compressed Natural Gas.
c_p; c_v = specific heat at constant pressure and constant volume [J/kg K].
d = cylinder bore [m]
E_p = a proportionality constant.
$error_T$ = error on the T_{IVC} evaluation [K].
$error_\rho$ = error on the compression ratio evaluation.
F = loss function [J/kg K].
G_{nozzle} = mass flow of the equivalent convergent nozzle [kg/s].
h = heat exchange coefficient between gas and chamber walls [W/m^2 K].
I = specific enthalpy of the gas [J/kg K].
IMEP = Indicated Mean Effective Pressure [bar].
IVC = Inlet Valve Closure.
k = the isentropic coefficient.
LPP = Location of Peak Pressure [CAD].
LTDC = Location of TDC [CAD].
m = mass of gas in the cylinder [kg].
m_1; m_2 = the compression and expansion polytropic coefficients at the pressure curve inflection points.
MAP = Manifold Absolute Pressure [bar].
p = in-cylinder gas pressure [bar].
p_{bias} = pressure bias error [bar].
P_{noise} = pressure value originated by noise [bar].
p_{out} = the ambient pressure [bar].
ppr = pulse per revolution.
R = gas constant [J/kg K].
S = the in-cylinder gas specific entropy [J/kg K].
T = the in-cylinder gas temperature [K].
TDC = Top Dead Centre.
T_{IVC} = gas temperature at IVC [K].
T_{max} = the in-cylinder gas maximum temperature [K].
T_{wall} = cylinder wall temperature [K].
u = specific internal energy of the gas [J/kg K].
u_m = mean piston speed [m/s].
V = cylinder volume [m^3].
v = specific volume of the in-cylinder gas [m^3/kg].
ω = the engine speed [rad/sec].
δF_1; δF_2 = *loss function* increments at the angular position ϑ_1 and ϑ_2 [J/kg K].
δF_{LPP} = the loss function increment at the peak pressure position [J/kg K].
δF_m = the mean value between δF_1 *and* δF_2 [J/kg K].
δm = the mass entering the cylinder during the crank rotation $\delta\vartheta$ [kg].
δp = pressure change due to a crank rotation $\delta\vartheta$ [bar].
δQ = heat received by the gas during the crank rotation $\delta\vartheta$ [J/kg].
δq = specific heat received by the gas during the crank rotation $\delta\vartheta$ [J/kg].
δS = specific entropy variation corresponding to a crank rotation $\delta\vartheta$ [J/kg K].
δV = volume change due to a crank rotation $\delta\vartheta$ [m^3].

GREEK SYMBOLS

ϑ_1; ϑ_2 = angular positions of the minimum and maximum relative volume change $\delta V/V$ [CAD].
$\Delta(\vartheta)$ = offset applied to the right segment of the pressure curve to compensate for heat transfer [bar].
ϑ = generic crank angle [CAD].
ϑ_0 = the middle of the right region of the pressure curve [CAD].
ϑ_{loss} = loss angle [CAD].
ϑ_{TDC} = the estimated TDC location [CAD].
$\delta\vartheta$ = 1 degree crank rotation [CAD].
η = coefficient depending on the heat transfer with chamber walls.
μ = rod to crank ratio.
ρ = engine compression ratio.